Journal of Hydraulic Research

ISSN: 0022-1686 (Print) 1814-2079 (Online) Journal homepage: http://www.tandfonline.com/loi/tjhr20

River morphodynamics with creation/consumption of grain size stratigraphy 1: laboratory experiments

Enrica Viparelli , Robert Haydel , Martino Salvaro , Peter R. Wilcock & Gary Parker

To cite this article: Enrica Viparelli , Robert Haydel , Martino Salvaro , Peter R. Wilcock & Gary Parker (2010) River morphodynamics with creation/consumption of grain size stratigraphy 1: laboratory experiments, Journal of Hydraulic Research, 48:6, 715-726, DOI: 10.1080/00221686.2010.515383

To link to this article: http://dx.doi.org/10.1080/00221686.2010.515383

Published online: 13 Dec 2010.

IAHR AIRH
Taylor & Francis
Taylor & Francis Group

Journal of Hydraulic Research Vol. 48, No. 6 (2010), pp. 715–726
doi:10.1080/00221686.2010.515383

Research paper

River morphodynamics with creation/consumption of grain size stratigraphy 1: laboratory experiments

ENRICA VIPARELLI, *Dipartimento di Ingegneria Idraulica ed Ambientale G. Ippolito, Università degli studi di Napoli Federico II, Naples, Italy; currently at Department of Civil and Environmental Engineering, University of Illinois Urbana-Champaign, 205 North Mathews Ave, 61801 Urbana IL, USA.*
Email: eviparel@illinois.edu (author for correspondence)

ROBERT HAYDEL, *Department of Civil and Environmental Engineering, University of Illinois Urbana-Champaign; currently at Construction Marker Data (CMD), New Orleans, LA, USA.*
Email: Haydelr@cdm.com

MARTINO SALVARO, *Dipartimento di Ingegneria Civile ed Ambientale, Dipartimento di Ingegneria Civile ed Ambientale, Università degli Studi di Trento, Italy.*
Email: martino.salvaro@ing.unitn.it

PETER R. WILCOCK, *Departments of Geography and Environmental Engineering, Johns Hopkins University, 21218 Baltimore MD, USA.*
Email: wilcock@jhu.edu

GARY PARKER, *Department of Civil and Environmental Engineering and Department of Geology, University of Illinois Urbana-Champaign, 205 North Mathews Ave, 61801 Urbana IL, USA.*
Email: parkerg@illinois.edu

ABSTRACT
Rivers with poorly-sorted bed sediment create their own stratigraphy as they deposit sediment. Prediction of the subsequent river degradation into its own deposit requires knowledge of the spatial structure of the grain size variation of the deposit. The ultimate goal of the present work is the development, testing and verification against experimental data of a numerical model of morphodynamics that can store stratigraphy into memory as it is created by aggradation, and can subsequently consume this stratigraphy if and when the river later degrades into the deposit. Such a morphodynamic model is tested using a surface-based bedload transport relation known to be applicable to the experiments considered here. Part 1 of a two-part paper addressing this issue describes the laboratory experiments and uses the experimental results performed at mobile-bed equilibrium to evaluate a bedload transport relation. In the companion paper, this bedload transport relation is installed into a morphodynamic model that specifically includes the creation/consumption of stratigraphy. The model is then tested against the experimental data.

Keywords: Bedload, hiding function, laboratory flume, mobile-bed equilibrium, sediment mixture, stratigraphy

1 Introduction

Gravel-bed rivers, and some sand-bed rivers, include a wide range of grain sizes in their bed and their transported sediment. As such rivers aggrade, they create a stratigraphic signature in terms of the spatial variation of the grain size distribution of their deposits. Rivers often degrade into the deposits that they have previously emplaced through aggradation. The time evolution of degradation thus depends upon, among other things, the previous aggradational history of the river.

Both experiments and numerical modelling were performed to characterize the vertical and streamwise grain size structure of the deposit emplaced by an aggrading stream carrying a wide range of sediment sizes (Spasojevic and Holly 1990, Hoey and Ferguson 1994, Cui *et al.* 1996, Seal *et al.* 1997, Toro-Escobar *et al.* 2000). Much less work, however, was done

Revision received 10 August 2010/Open for discussion until 30 June 2011.

ISSN 0022-1686 print/ISSN 1814-2079 online
http://www.informaworld.com

towards the development of a numerical model capable of storing into memory the spatial variation of the deposit created by aggradation in a way that can be re-accessed as the stream degrades into it. While Spasojevic and Holly (1990) or Cui *et al.* (2006a, 2006b) have developed such models, their ability to handle stratigraphy has not been tested and verified against detailed experiments. The only cases known to the authors of morphodynamic models that are able to store and access the stratigraphy and that have been validated against experimental data are presented by Ribberink (1987) and Blom (2008). While these works focus on the dune regime, this research fills this gap for the lower regime plane bed.

Models of river morphodynamics are useful tools to describe the evolution in space and time of a river, and to predict the consequences of natural events or human activities on the river system. These models are composed of several procedures to compute flow parameters, sediment transport and bed evolution in space and time (Armanini and Di Silvio 1988, Holly and Rahuel 1990a, 1990b, Wright and Park 2005a, 2005b, Blom 2008). Depending on the case of interest, the sediment can be considered to be either uniform or a mixture of different grain sizes.

If the sediment is approximated as uniform, it is generally characterized by a single characteristic diameter – i.e. the median, the geometric or the arithmetic mean of its grain size distribution – to compute sediment transport. A second, coarser diameter, generally of size D_{90} (such that 90% is finer), may be used to evaluate the roughness height. In morphodynamic models of bed evolution based on the assumption of uniform sediment, these parameters, once selected, are not allowed to vary in space and time (Parker 2004).

If the sediment is modelled as a mixture, the problem becomes more complex because (a) the grain size distribution of the bed surface may vary in space and time, (b) the interaction between the bed and the bedload must be considered and (c) the sediment transport must be computed on a grain-size-specific basis. Most methods used to describe the interaction between bed and bedload employ a form of the active layer approximation introduced by Hirano (1971). In the simplest of these models, the bed is divided into two regions: substrate, whose particles cannot be directly entrained into bedload, and active or surface layer, whose particles do exchange with the bedload (Parker 1991a, 1991b). The grain size distribution in the substrate can vary in the vertical direction, but does not vary in time. The substrate can be modified, however, via bed aggradation and degradation. The grain size distribution of the surface layer has no vertical structure, but can vary in time as grains exchange with the bedload. In surface-based models, the bedload transport rate and its grain size distribution are usually computed as functions of the grain size distribution of the surface layer and the applied hydraulic conditions (Parker 2004).

This research presents an extensive data set of flume experiments that characterize (1) lower regime plane bed equilibrium transport of mixtures of pea gravel and sand, (2) evolution towards equilibrium as well as the equilibrium steady state, in terms of measurements of the evolution of the bed profile and of the grain size distribution of the bed surface, and (3) creation/consumption of stratigraphy under non-equilibrium conditions (bed aggradation/degradation). This data set can be used to test existing and new morphodynamic modes for lower regime plane bed with non-uniform sediment. These experiments are used to develop a bedload transport relation for mixtures of pea gravel and sand that is known to apply for a range of conditions in the specific flume considered here. In the companion paper (Viparelli *et al.* 2010), (a) this transport model is incorporated into a numerical model of river morphodynamics that specifically includes the creation and consumption of stratigraphy, and (b) the model is tested against the same experimental data as presented herein.

Rather than to develop a completely new bedload relation, the analysis here is done in the context of the simplest possible set of modifications to the well-known bedload transport relation of Ashida and Michiue (1972) derived for sand and pea gravel, i.e. the size range used in the experiments described below. This is done in part because most of the sediment relations for mixtures (Parker 1990, Wilcock and Crowe 2003) are derived specifically for gravel-bed streams with grain sizes that are substantially coarser than those considered here.

It is reasonable to ask why a "new" bedload transport relation is developed here, if a wide range of existing models are available (e.g. as listed by Garcia 2008). The necessity for such a relation is rooted in the need for verification of the morphodynamic model presented in the companion paper. If the morphodynamic model is inadequate to handle the creation/consumption of stratigraphy observed in flume experiments, the reason for the failure might be due to one of two possibilities. The morphodynamic model itself may be flawed, or the model itself may be essentially correct, but the bedload transport rates and size distributions may be incorrectly predicted by the bedload transport relation used in the model. Here the second possibility is eliminated by computing the bedload transport rate and its grain size distribution with a relation derived from conditions of mobile-bed equilibrium obtained in the same flume, with the same sediment mixture, and within the same range of conditions that have been used to perform the experiments to test the model against observed morphodynamic/stratigraphic changes. There is, indeed, a third potential cause for the deviation between measured and the predicted data, i.e. the grain friction model, as pointed out by Ribberink (1987). The comparison between our data and two more extensive data sets is presented in Fig. 3 of the companion paper to show that the grain friction model embedded in the code reasonably reproduces the experimental data. This exercise eliminates this third possibility.

The present research was motivated by the StreamLab06 facility at St Anthony Falls Laboratory, University of Minnesota, USA (Wilcock *et al.* 2008). This large flume operates in a water-feed, sediment-recirculating mode and allows for field-scale studies on gravel transport in rivers. Examples of such studies

are those presented by Singh *et al.* (2009) and Ganti *et al.* (2009). The facility is of such a large scale, however, that studies on (a) evolution of stratigraphy and (b) approach to mobile-bed equilibrium are difficult to perform. The experiments described herein were motivated by the larger-scale experiments performed in Minneapolis, so as to achieve both of these objectives in the "mini StreamLab" facility described below. Both of these research programmes are parts of a multidisciplinary effort undertaken by the National Center of Earth-Surface Dynamics.

2 Overview on experiments

The laboratory experiments were conducted at the Hydrosystems Laboratory of the University of Illinois at Urbana, Champaign, in a flume of water-feed and sediment-recirculating configuration. The sediment transport regime was – in all cases – lower-regime plane bed. During each experiment, longitudinal profiles and water surface elevations were periodically measured so as to determine if the flow and sediment transport rate had reached equilibrium. The definition of equilibrium in a river or in a flume is a delicate matter because it depends on the particular scale of the problem and on the available measurements. In most cases, it can be defined as a state in which all the hydraulic parameters, such as channel slope and sediment transport rate, vary around a mean value that appears to be constant in time and space (Blom *et al.* 2006).

Nine different runs were performed for different values of (a) constant water discharge and (b) water surface elevation at the downstream flume end. These two parameters control the equilibrium reached in a water-feed and sediment-recirculating flume (Parker and Wilcock 1993). If the flow and the sediment transport were deemed to have attained equilibrium, the sediment transport rate and its grain size distribution were measured. The flow was stopped, and the bed surface was sampled and sieved at different locations. The sampled surface sediment was then placed back in the flume at the place where the sample was taken, and a new run started. That is, the sediment of the bed deposit was not removed or remixed (other than the samples themselves) in proceeding from run to run. At the end of Run 9, core samples were taken at 10 different cross-sections to measure the spatial (vertical and streamwise) structure of the grain size distribution of the deposit.

As noted above, the bedload transport relation obtained from the experiments reported here has the same structure as that of Ashida and Michiue (1972) for sediment size mixtures. The bedload transport rate for each grain size range was computed as a function of the excess of shear stress above a critical value that varies for each grain size range, as well as the availability of that size range in the active layer. These critical values were computed by considering the different mobility of coarse and fine particles as quantified by a hiding function. Coarse grains are more difficult to move because they are heavier than fine grains. These same coarse grains, on the other hand, tend to hide fine grains that so become harder to move. The result of these two opposite effects is that the mobility of coarse grains is modestly elevated compared with a uniform sediment composed of the coarse size only. Fine grains are still more mobile than coarse grains, even if their mobility decreases compared with a uniform sediment of similar size (Parker and Klingeman 1982b). The main difference between the bedload relation derived below and the original version from Ashida and Michiue (1972) concerns the hiding function. More specifically, the hiding function of the original formula predicts a higher sediment transport rate with a size distribution that is finer than that of the bedload measured during the experiments. Appropriate adjustments were thus made to bring the predictions in accord with the data.

3 Experimental set-up

Experiments were performed in a water-feed, sediment-recirculating flume. This configuration is more convenient than a sediment-feed flume to run experiments with poorly-sorted sediment, because the mixture can be prepared and put in the flume just once (Parker *et al.* 1982a). The total amount of sediment in a water-feed and sediment-recirculating flume is constant, and the transition between one and another equilibrium state is characterized by the redistribution of the sediment. For example, once the bed equilibrates with a slope S_1, the water discharge is changed so that the bed will tend to a new condition of equilibrium characterized by the new slope S_2. If $S_2 > S_1$, the difference in elevation between the up- and downstream ends of the flume must increase, with erosion in the downstream half and deposition in upstream half. On the contrary, if $S_2 < S_1$, the difference in elevation between the two flume ends must decrease, with consequent erosion in the upstream part and deposition in the downstream part.

For the experiments described below, the horizontal flume bottom was covered with an 18.5 cm thick layer of the poorly sorted mixture of gravel and sand represented in Fig. 1. The initial grain size distribution was measured at 6 flume sections to verify its uniformity and then the tests started. The first

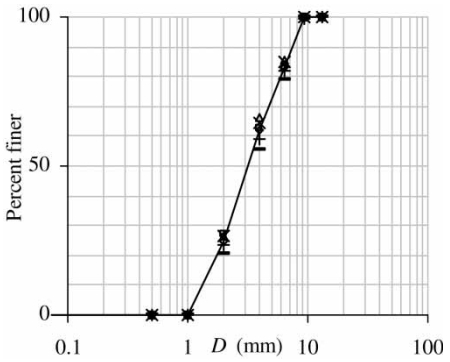

Figure 1 Grain size distribution of sediment used during experiments (C1). (◇) $x = 1$ m, section (□) 1, (△) 2, (×) 3, (+) 4, (−) 5

sample was taken at $x = 1$ m, where x represents streamwise coordinate measured from the upstream flume end. The other samples were taken at five test sections: Section 1 at $x = 2.5$ m, Section 2 at $x = 4.3$ m, Section 3 at $x = 6.5$ m, Section 4 at $x = 8.5$ m and Section 5 at $x = 10.5$ m. The samples were taken using a cylinder of 0.0508 m (2 in.) diameter, inserted into the flume bed at its transversal centre. The sediment in each sample was taken to a depth of 15 cm. As seen in Fig. 1, the parent sediment mixture is uni-modal, consisting of about 25% sand and 75% pea gravel. The geometric mean and median diameters are near 3.20 mm, $D_{90} = 7.47$ mm and the geometric standard deviation $\sigma_g = 1.81$. The sediment density was $\rho_s = 2580$ kg/m^3.

Two other sampling techniques will be described below, i.e. surface sampling and core sampling of the bed. To clearly distinguish between the different sampling methods, the following abbreviations are introduced: C1 for bulk sampling with the cylinder (i.e. 2 in. pipe), C2 for surface sampling and C3 for core sampling to measure stratigraphy.

The flume was straight, with a rectangular cross-section, a plexiglas wall on the left-hand side and a plywood wall on the right. The latter was installed to narrow the width of the mobile-bed reach from 0.91 m (3 ft.) to 0.61 m (2 ft.) to produce a width/depth ratio typical of lower regime plane bed without alternate bars. The mobile-bed reach was 11.8 m long, extending from the end of the recirculating line to the wooden sediment trap at the downstream end. The sediment collected in the trap entered the recirculating line and was pumped to the upstream flume end with a diaphragm pump. Particles coarser than 6.5 mm were manually recirculated, because the diaphragm pump would clog with such coarse material. The frequency of this action depended on the sediment transport rate, i.e. coarse sediment was continuously collected during the runs in a small bucket, and if the bucket was half-full, the sediment was fed at the upstream flume end. Water surface elevations were controlled by a rectangular tailgate, i.e. a weir, at the downstream flume end. Water discharge was measured with two electromagnetic flow meters – one on the recirculating line and the other on the pipe from the laboratory head tank.

Water elevation was measured in the test sections with piezometers. Longitudinal profiles were measured with ultrasonic transducer probes described by Wong *et al.* (2007). These were taken from $x = 2.5$ m to $x = 10.5$ m; the flume sidewalls in the first 2.5 m were too high to use the ultrasonic probes. Four probes were placed on the same cart and four longitudinal profiles were simultaneously recorded by measuring bed elevation each 0.40 m for 30 s each. The average longitudinal profile resulted then from these four profiles.

4 Experimental procedure

The channel was backfilled with a hose. As the bed was saturated, water was introduced from the head tank. The recirculating pump was turned on and the discharge from the head tank was adjusted to the desired value. The tailgate was lowered to fix the water elevation at the downstream flume end. Water surface and bed elevations were measured each one or two hours. In these runs, it was assumed that the flow and the sediment transport reached equilibrium as the longitudinal bed profile was nearly constant for two or three consecutive measurements. At mobile-bed equilibrium, the sediment transport rate was measured. This was done by opening the bypass on the recirculating line and diverting the water and sediment into a clean garbage can where the sediment was collected. During this period, the discharge from the head tank was adjusted to account for water loss from the recirculating line. Coarse sediment was manually removed from the sediment trap. After a 5–15 min interval, depending on the sediment transport rate, the bypass was closed and the experiment terminated. The entire sample was dried in an oven, weighed and sieved. A final longitudinal profile was measured, and the bed was drained of water.

Surface samples were collected at the five measuring sections (C2) with a procedure based on Klingeman and Chaquette's field method (Klingeman *et al.* 1979). To do this, a rectangular area approximately 0.20 m long in the streamwise, and 0.30 m wide in the transverse direction and transversely centred in the flume was demarcated. The coarsest exposed particle was then removed. The surface was spooned down to a level corresponding roughly to the hole bottom created by removing the largest exposed grain (Parker 1990). Samples were oven-dried and sieved. They were then replaced at the sampling sites, and a new run was commenced.

At the end of the ninth run, the bed was sampled with a metal box especially designed for sampling the vertical stratigraphy (C3). The box, 0.30 m high with a rectangular base 0.15 m long and 0.10 m wide, is described by Blom *et al.* (2003). The flume was backfilled with a hose, and the metal box was driven into the bed. A metal plate was then pushed under the box, and both parts were then simultaneously removed. Between the eighth and the ninth run, the bed slope was increased by sediment deposition in the upstream flume portion and erosion in the downstream portion, because the experiments were conducted in a water-feed and sediment-recirculating flume. Vertical sorting was thus observed mainly in the upstream flume portion where the aggradation took place, while in the downstream flume portion, most of the previously deposited material was eroded. The bed was sampled each 0.50 m from $x = 0.5$ m to $x = 3$ m, then each metre at $x = 4$ m and $x = 5$ m and finally each 2 m at $x = 7$ m and $x = 9$ m. At each section, one core sample was taken on the left side and another on the right flume side (C3). Each core was then sliced into layers of a thickness of 0.01 m with a metal plate. Each layer was oven-dried and sieved. To characterize the vertical stratigraphy at each section, the grain size distributions of samples from the same layer taken from the left- and right-hand sides were averaged.

5 Experimental results

The experimental runs are described in Table 1 in terms of water discharge and downstream water elevation, because in a water-feed and sediment-recirculating flume, the condition for equilibrium for poorly-sorted sediments depends on these two parameters and on the grain size distribution of the bed surface layer (Parker and Wilcock 1993). The duration of each run is reported in the last column of Table 1. This parameter is used in Viparelli *et al.* (2010) to perform numerical simulations and to define the numerical condition of equilibrium. This condition will be defined by considering Runs 6–9 only because the first five runs were characterized by continuous problems with the pump, i.e. frequent clogging and water in the line of the compressed air. The bed at the beginning of Run 1 was horizontal with no vertical stratigraphy, i.e. a grain size distribution that was as uniform as possible in the horizontal and vertical directions. The initial conditions for Runs 2–9 were the longitudinal profile and the bed at the end of the previous run.

In a water-feed and sediment-recirculating flume, where the total amount of sediment in the system is constant, the bed surface and the substrate are segregated from the same parent mixture (Parker *et al.* 1982a). As a result, if the (relatively thin) bed surface equilibrates to a value that is noticeably coarser than the initial mixture, the much thicker substrate should be slightly finer in the aggregate than the initial mixture.

The longitudinal profiles recorded at mobile-bed equilibrium for all experiments are reported in Fig. 2. Also included is the initial bed, represented as a dash-dot black line. In the insets of the left corner, the change in elevation relative to the previous steady state, denoted as $\Delta\eta$, is represented to clearly show where the bed material was eroded or deposited in the transition from one condition of equilibrium to the other. It is observed that the flow and the sediment transport reached different conditions of equilibrium corresponding to the different imposed constraints described in Table 1. The change from one equilibrium to the next was accomplished by redistributing the sediment in the flume. This redistribution can be seen in Fig. 2 by comparing, for example, the profiles of Runs 3 and 4. The steepest of all bed slopes, and thus the lowest bed elevation at the downstream flume end, resulted in Run 3. In progressing from Run 3 to Run 4, the bed slope decreased, and the bed equilibrated via deposition in the downstream flume portion and erosion in the upstream portion. The bed slope further decreased in Runs 5 and 6, again with erosion of sediment in the upstream flume portion and deposition downstream. During Run 7, the bed slope increased due to erosion in the downstream flume half and deposition in the upstream half. The new deposit so created in the upstream half was partially eroded during Run 8, during which the bed slope decreased again. Finally, in progressing from Runs 8 to 9, the bed slope increased, with deposition in the upstream flume portion and erosion downstream.

The morphodynamic regime in all the runs was lower regime plane bed; therefore no bedforms and no significant lateral

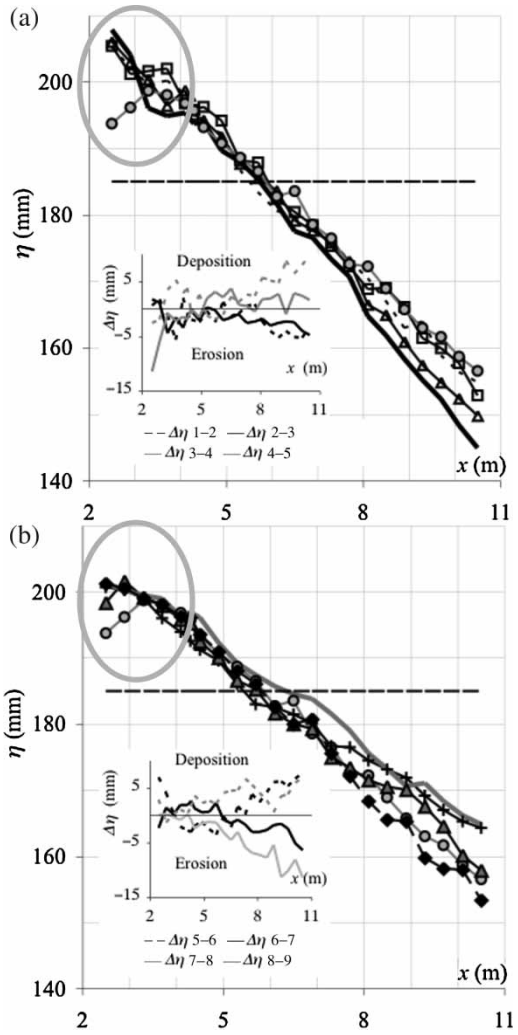

Figure 2 Longitudinal bed profiles at equilibrium recorded during Runs 1–5 in Fig. 2(a) and Runs 5–9 in Fig. 2(b). (—) Profile for Run 3 (steepest slope) in Fig. 2(a), (——) profile for Run 8 (mildest slope) in Fig. 2(b) and (−◆−) profile for Run 9 (final profile) in Fig. 2(b). Insets show net variation of bed elevation $\Delta\eta$ observed during Runs 2–9. (o) area with significant entrance effects. (— –) initial bed, Run (– □ –) 1, (–△–) 2, (—) 3, (- -) 4, (–•–) 5, (+) 6, (–▲–) 7, (—) 8, (–◆–) 9

Table 1 Description of runs with Q (water discharge set by pump) and ξ_w (water elevation at downstream flume end set by tailgate)

Run	Q (l/s)	ξ_w (cm)	Run duration (h)
1	30	22	24.67
2	25	21	12.08
3	20	19	15.33
4	35	23	6.25
5	20	21	16.50
6	30	24	7.42
7	30	23	10.75
8	35	24.8	6.50
9	35	22.5	5.75

variation of bed elevation was observed except in the very upstream flume portion, where entrance effects due to flume narrowing caused a scour on the left-hand side of the cross-section. Entrance effects can be clearly observed in the longitudinal profiles of Fig. 2 in the grey circles of Runs 3, 5 and 7. The only migrating form that was observed appeared at the beginning of the runs, as significant erosion was observed at the downstream flume end and sediment was deposited upstream in a small delta front that started migrating downstream. Unfortunately, no data are available to reconstruct the longitudinal profile of the bed deposit in the farthest upstream flume portion. Entrance effects caused a strong local spatial variation in bed elevation in the upstream flume portion, i.e. around and upstream of Section 1 at $x = 2.5$ m. This effect never propagated farther downstream than $x = 3$ m. With this in mind, the bed shear stress was computed by considering channel slopes and water depths at equilibrium in the flume portion that was not affected by the entrance region, i.e. from Section 2 at $x = 4.3$ m to Section 5 at $x = 10.5$ m.

The sieve analysis of surface samples (C2) showed a systematic coarsening of the bed surface along the entire flume length towards the end of each run. This is shown in Table 2, where the geometric mean diameter of the bed surface is reported. This coarse pavement acts to protect smaller grains, which so become harder to move.

Figure 3 shows the grain size distribution of the initial parent mixture as well as all the surface grain size distributions measured at equilibrium at the end of the nine runs. These surface grain size distributions were determined by averaging samples over the flume length, because the streamwise variation of grain size distribution of the bed surface, if it occurs, was essentially due to data scatter. The surface layer was always coarser than the initial mix; its grain size distribution was similar in all runs except for Run 2, 5 and 6. In Run 2, the average grain size distribution of the surface layer was finer than in all the other runs, whereas in Runs 5 and 6, for which the equilibrium sediment transport rate was very low (Table 3), the resulting bed surface was noticeably coarser.

In interpreting these results, it should be borne in mind that the surface samples were obtained by scraping off surface material with a spoon (C2), and as such have a somewhat different status from the volumetric samples used to characterize the bulk material (C1) (Fripp and Diplas 1993). A comparison between different samples of the parent material taken with the two methods is also shown in Fig. 3 ("PM C1" and "PM C2"). Samples obtained by spooning unarmoured bed material (C2) are somewhat coarser than the volumetric samples (C1), but they are finer than any of the nine samples characterizing the bed surface collected at the end of each run (C2). In consequence, samples obtained from the surface by spooning (C2) can be used to characterize whether or not the surface is armoured compared with the parent material.

The sieve analysis of core samples (C3) at the end of Run 9 revealed a substrate that was nearly equal to, or slightly coarser (mainly in the upper layers) than, the original mixture

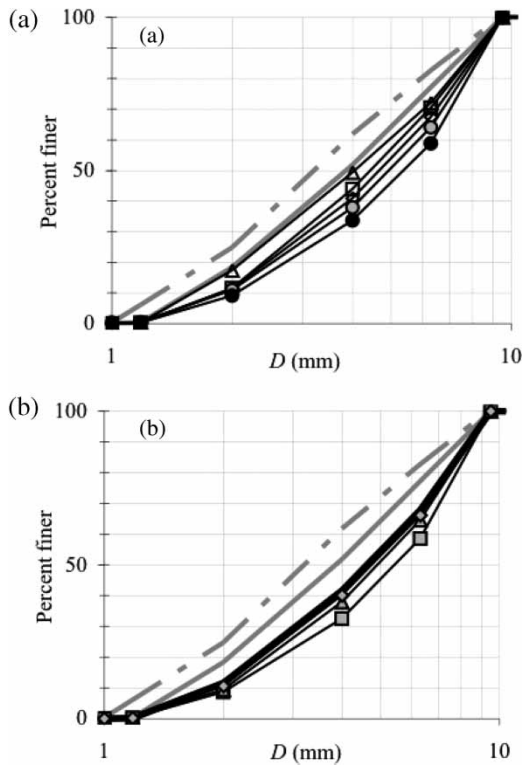

Figure 3 Comparison between parent mixture and grain size distribution at equilibrium averaged over flume length in nine runs. "PM C1" refers to bulk volumetric sampling of parent material (C1) while "PM C2" to samples of parent material taken by scraping off surface material with spoon (C2). Grain size distribution of bed surface at equilibrium (C2) is plotted with grain size distribution of parent material for Runs 1–5 in (a) and for Runs 6–9 in (b). (— –) PM C1, (—) PM C2, Run (– □ –) 1, (–△–) 2, (–◇–) 3, (–o–) 4, (–●–) 5, (–■–) 6, (–▲–) 7, (–◆–) 8, (—) 9

Table 2 Geometric mean diameter of bed surface in (mm)

Run	1	2	3	4	5	6	7	8	9
Section 1	4.13	3.56	4.74	4.69	4.11	4.89	4.33	4.44	4.19
Section 2	4.47	3.73	3.87	4.40	4.68	4.86	4.45	3.81	4.33
Section 3	4.08	3.80	4.23	4.00	4.77	4.62	4.53	4.49	4.09
Section 4	3.93	4.05	4.32	4.45	4.79	4.60	4.44	4.10	4.31
Section 5	4.06	4.06	4.21	4.55	5.08	4.69	4.47	4.85	4.19

Note: For reference, geometric mean diameter of parent mix was 3.19 mm.

Table 3 Bedload transport rates and characteristic diameters at equilibrium

Run	G_s (g/min)	H (cm)	S (m/m)	τ_b (Pa)	D_{lg} (mm)	D_{l90} (mm)
1	731	7.6	0.0069	4.90	3.31	7.43
2	491	6.8	0.0073	4.68	3.78	7.93
3	458	5.9	0.0079	4.42	3.51	7.62
4	1432	8.3	0.0069	5.33	3.70	7.74
5	54	6.1	0.0063	3.62	2.85	6.79
6	64	8.2	0.0046	3.48	3.36	7.69
7	371	8.0	0.0060	4.48	3.89	7.83
8	151	8.7	0.0052	4.16	2.99	7.58
9	1068	8.2	0.0069	5.26	3.66	7.93

Notes: G_s, sediment transport rate (g/min); H, water depth averaged over flume length; S, bed slope averaged over flume length; τ_b, computed shear stress in bed region; D_{lg}, geometric mean diameter of bedload; D_{90}, diameter such that 90% of bedload is finer. For reference, the geometric mean diameter of parent mix was 3.19 mm.

(C1). This unexpected result is explained, considering that at the end of each run the bed was drained to sample the surface, and then was saturated again. The procedure was necessary to sample the surface, but it may have caused a modest reworking of the bed, with some of the finer material transported and trapped in the deeper portion of the bed deposit.

Coarsening of the surface was evident in all runs, but in Run 9, the surface sample (C2) is seen to be much coarser than the first layer of the core sample (C3). This difference can be again partly ascribed to the difference in the sampling technique (i.e. spooning of bed surface for C2, and bulk samples for bed deposit C3). More specifically, the first layer of each core sample consisted of sediment from both the surface layer and the topmost substrate portion. As a result, samples so obtained should be considered to be a mixture of the somewhat coarser sediment of the surface and the finer sediment of the topmost substrate portion. For details, see the Excel file *miniStreamlab-Data.xls* at http://hdl.handle.net/2142/15496.

In Table 3, the sediment transport rates, water depths and channel slopes at equilibrium are reported along with some characteristic bedload diameters. The bed shear stresses were computed by removing the sidewall effects using the procedure of Vanoni and Brooks (Vanoni 1975). The cross-section was divided into two non-interacting portions, i.e. the bed and the wall region. The energy gradient and mean flow velocity were assumed to be identical in both regions, equal to the energy slope and the mean flow velocity of the entire cross-section. It was then assumed that a resistance relation of Darcy–Weisbach type applies to the entire cross-section as well as in the wall and in the bed regions. Considering that the walls are smooth compared with the mobile bed, the friction coefficient for the wall region was computed with Nikuradse's relation for smooth pipes. The shear stress in the wall region was evaluated multiplying the friction coefficient, the density of the water and the square of the mean flow velocity (e.g. Eq. (3) of companion paper). The shear stress in the bed region was finally computed from the equation of conservation of downstream momentum (e.g. Eq. (4) of companion paper).

Sieve analyses of the bedload samples indicated that bedload had a grain size distribution similar to the initial mixture except during Run 5 and Run 8, which were characterized by fine geometric mean sizes and low sediment transport rates (54 and 151 gr/min, respectively). Apparently at such low transport rates, not all particles were moved, resulting in partial transport (Wilcock and McArdell 1993). The bedload measured during Run 6, also characterized by a low sediment transport rate of 64 g/min, had a grain size distribution similar to that of the substrate. The reason for this is not known, but it may – in part – reflect experimental error related to the manual recirculation of the coarse fractions.

6 Bedload relation

Bedload relations for uniform material generally compute the sediment transport rate as a function of flow parameters, such as the mean flow velocity or the shear stress. Many bedload relations empirically relate a non-dimensional bedload transport rate per unit width known as the Einstein parameter q_b^*, with the non-dimensional shear stress or Shields parameter τ_b^*, where

$$q_b^* = \frac{q_b}{\sqrt{RgDD}} \tag{1a}$$

$$\tau_b^* = \frac{\tau_b}{\rho RgD} \tag{1b}$$

in which q_b = bedload volume transport rate per unit width, R = submerged specific sediment gravity and D = characteristic sediment diameter. The general form of such a bedload relation is

$$q_b^* = \mathrm{f}(\tau_b^*) \tag{2}$$

$$q_b^* = \mathrm{f}(\tau_b^* - \tau_c^*) \tag{3}$$

where τ_c^* is the critical or threshold value of Shields number (Wong 2003, Wong and Parker 2006), which can be defined

either to provide a fit of data or to characterize a lower limit for significant transport (Parker 2004).

If sediment transport is modelled as a mixture of different grain sizes, the interaction between the bed surface and the bedload must be considered. This process has a stochastic nature (Wong *et al.* 2007) because the probability for a particle to be entrained into bedload decreases with its depth in the bed or diameter. Despite Parker *et al.* (2000) developed a probabilistic formulation to describe this phenomenon, such a formulation is not yet easily implemented. As a result, the active layer approximation proposed by Hirano (1971) was used. The active or surface layer is defined to be a thin region in the upper bed portion where sediment grains have an equal and finite probability in time to be entrained into bedload, and the grain size distribution was assumed not to vary in the vertical direction. The substrate is the whole bed under the active layer, where the grain size distribution may vary in the vertical, but where the probability of a grain to be entrained into bedload is assumed to be zero.

Let q_{bi} = bedload transport rate in the ith size range, which has characteristic grain size D_i. The total bedload transport rate q_{bT} is defined as sum of q_{bi} over all grain size ranges

$$q_{bT} = \sum_{i=1}^{N} q_{bi} \tag{4}$$

The fraction of bedload material in each grain size range p_i is consequently

$$p_i = \frac{q_{bi}}{q_{bT}} \tag{5}$$

For each grain size range, a Shields and Einstein number can be defined as

$$q_{bi}^* = \frac{q_{bi}}{\sqrt{RgD_i}D_iF_i} \tag{6a}$$

$$\tau_{bi}^* = \frac{\tau_b}{\rho RgD_i} \tag{6b}$$

and a functional relation like in Eqs. (2) or (3) (i.e. $q_{bi}^* = \mathrm{f}(\tau_i^*)$ or $q_{bi}^* = \mathrm{f}(\tau_i^* - \tau_{ci}^*)$) can be assumed. Note that F_i represents the fraction of surface layer material in the ith grain size range. Equations (2) or (3) and (6a,b) define a surface-based bedload relation, because this inclusion of parameter F_i in the denominator of Eq. (6a) implies that a size range not in the surface layer is not available to be transported as bedload.

The surface-based version of the relation of Ashida and Michiue (1972), Eq. (7) below, was tested against the present laboratory data. This relation has the structure of Eq. (3). The surface grain size distributions measured at equilibrium were used to compute q_{bi} from Eqs. (6a,b) as

$$q_{bi}^* = 17\left(\tau_i^* - \tau_{ci}^*\right)\left(\sqrt{\tau_i^*} - \sqrt{\tau_{ci}^*}\right) \tag{7}$$

The critical value of the Shields parameter for each grain size range was evaluated using

$$\frac{\tau_{ci}^*}{\tau_{scm}^*} = \mathrm{f}\left(\frac{D_i}{D_{sm}}\right) = \begin{cases} 0.834 \cdot \left(\dfrac{D_i}{D_{sm}}\right)^{-1} & \text{for} \dfrac{D_i}{D_{sm}} \le 0.4 \\ \left[\dfrac{\log(19)}{\log\left(19\dfrac{D_i}{D_{sm}}\right)}\right]^2 & \text{for} \dfrac{D_i}{D_{sm}} > 0.4 \end{cases} \tag{8}$$

where D_{sm} is the arithmetic mean diameter of the grain size distribution of the surface layer and $\tau_{scm}{}^*$ the reference Shields number, taken to 0.05. In implementing Eqs. (7) and (8) to compute the effective value of the Shields parameter for each grain size range $\tau_{ci}{}^*$, and the volume bedload transport rate for unit width for each grain size range, the measured grain size distributions of the surface layer were averaged over the flume length to have a single value of the surface geometric mean diameter and a single grain size distribution for each condition of equilibrium. Figure 4 compares the measured transport rates (summed over all grain sizes) in grams per minute for all nine experiments versus the transport rate (summed over all grain sizes) predicted directly from the relation of Ashida and Michiue (1972). The equation over-predicts the bedload transport rate by slightly more than a factor of 2. A linear regression indicates that the measured transport rates are about 40% of the predicted rates.

This result is not unexpected. Wong and Parker (2006) re-analysed the bedload transport equation of Meyer-Peter and Müller (1948) in the context of a subset of the data they themselves used

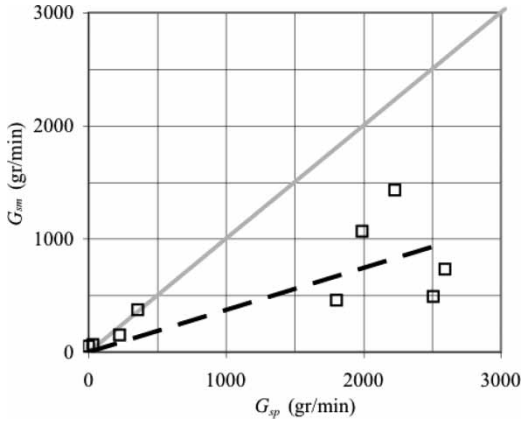

Figure 4 Comparison between predicted and measured sediment transport rates G_{sp}, and G_{sm}, predictions from Eqs. (7) and (8). (□) Data, (—) perfect equality, (– –) linear regression

to derive their equation. This subset pertained to uniform sediment transported under plane-bed conditions. They found the equation to over-predict the bedload transport rate by a factor of 2. Parker (2008) compared the relations of Einstein (1950) and Ashida and Michiue (1972) to the same data set, and again found an over-prediction by a factor of 2. Thus the over-prediction obtained here for the relation of Ashida and Michiue (1972) as applied to mixtures follows the same trend as was found for uniform sediment.

Figure 5 shows the ratio D_{lp}/D_{lm}, where D_{lp} is the predicted geometric mean of bedload and D_{lm} the corresponding measured value, for all nine experiments. The predicted values are again from the relation of Ashida and Michiue (1972). Overall, the predicted geometric mean size of the bedload is about 71% of the measured value (i.e. $D_{lp} = 0.71\, D_{lm}$). For Run 5, the relation predicted vanishing load. If this run were removed, the corresponding predicted size is about 80% of the measured value. The relation of Ashida and Michiue (1972) is clearly not wildly off. If it were to be used in the test of the stratigraphy/tracking model described by Viparelli *et al.* (2010), however, substantial error would result, not necessarily because stratigraphy is tracked incorrectly but because of the systematic error in the prediction of bedload transport. With this in mind, an adjusted version of the relation was developed so as to specifically apply to mobile-bed equilibrium conditions of the present experiments.

The hiding function in Eq. (8) is shown in Fig. 6. Also shown are two useful limiting cases, i.e. size independence and equal mobility. These two are easily expressed in terms of a power

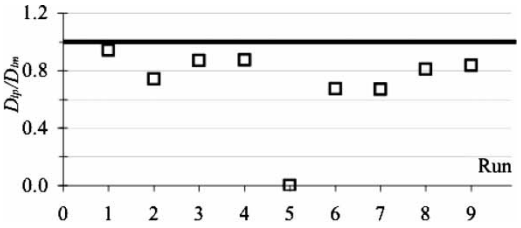

Figure 5 Comparison between (−) predicted and (□) measured geometric mean diameter in sediment load; predictions from Eqs. (7) and (8)

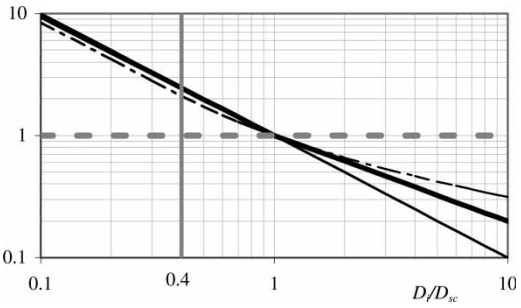

Figure 6 Hiding functions, where D_{sc} is the characteristic diameter of surface layer (e.g. median, arithmetic or geometric mean). (— –) Ashida and Michiue, (—) Eq. (10), (—) equal mobility, (– –) size independence and (—) $D_i/D_{sc} = 0.4$

relation introduced by Parker and Klingeman (1982b) as

$$\frac{\tau^*_{ci}}{\tau^*_{c50}} = \left(\frac{D_i}{D_{50}}\right)^{-m} \tag{9}$$

Here, D_{50} is the median size (of either surface or substrate sediment, as appropriate), $\tau_{c50}{}^*$ the corresponding critical Shields number and m the exponent between 0 and 1. In the context of this analysis, however, D_{50} and $\tau_{c50}{}^*$ could be replaced by values based on the arithmetic or geometric mean of the surface or substrate sediment.

In Figure 6, $m = 0$ corresponds to the limiting case of size independence where all particles are mobilized at the same Shields number, the hiding effect is absent and the beginning of motion linearly depends on the grain size. The other limit $m = 1$ corresponds to equal mobility, according to which the critical Shields number varies linearly with grain size and all particles are mobilized at the same shear stress. Field and laboratory data suggest behaviour closer to the case of equal mobility rather than size independence, but the exponent m nevertheless tends to be smaller than unity (Parker 2004, Garcia 2008).

The hiding function of Ashida and Michiue (1972) in Fig. 6 suggests that the deviation from equal mobility is weaker for finer, and stronger for coarser grain sizes. This further suggests the use of a modified form of Eq. (9) that has two values of m, i.e. a larger value for finer, and a smaller for coarser grain sizes. With D_{sg} being the surface geometric mean sediment size, the following hiding function was developed based on the above data:

$$\frac{\tau^*_{ci}}{\tau^*_{scg}} = \begin{cases} \left(\dfrac{D_i}{D_{sg}}\right)^{-0.98} & \text{for } \dfrac{D_i}{D_{sg}} \le 1 \\ \left(\dfrac{D_i}{D_{sg}}\right)^{-0.68} & \text{for } \dfrac{D_i}{D_{sg}} > 1 \end{cases} \tag{10}$$

Note that in contrast to the hiding relation of Ashida and Michiue (1972), Eq. (10) uses D_{sg} rather than D_{sm}. This hiding function is also shown in Fig. 6. The value of $\tau^*{}_{scg}$ estimated by eye was $\tau^*{}_{scg} = 0.043$. The hiding function of Eq. (10) was then embedded into a modified Ashida–Michiue equation as

$$q^*_{bi} = 17\alpha\left(\tau^*_i - \tau^*_{ci}\right)\left(\sqrt{\tau^*_i} - \sqrt{\tau^*_{ci}}\right), \tag{11}$$

where α is the coefficient adjusted to fit the data. A linear regression resulted in $\alpha = 0.270$. Figure 7 compares the measured transport rates (summed over all grain sizes) for all nine experiments versus the transport rate (summed over all grain sizes) predicted from Eqs. (10) and (11). A comparison of Figs. 4 and 7 indicates improved accuracy of prediction resulting from the modified formulation. The overall mean value of the coefficient of the linear regression between measured and predicted bedload transport rates is 0.996. The points in Fig. 7 that are relatively far from the line of perfect

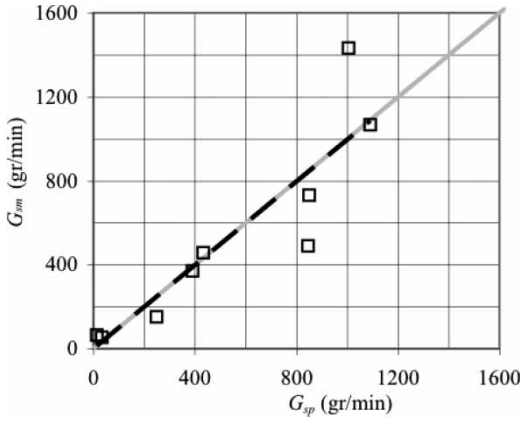

Figure 7 Comparison between predicted G_{sp} and measured G_{sm} sediment transport rate using Eqs. (10) and (11). (□) Data, (—) perfect equality, (– –) linear regression

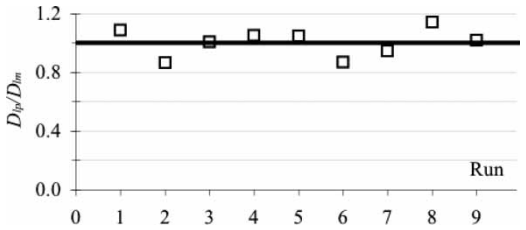

Figure 8 Comparison between (−) predicted and (□) measured geometric mean diameter in sediment load; predictions from Eqs. (10) and (11)

agreement are those pertaining to Runs 2 and 4. During these runs, the measurements might have been affected by problems with the recirculating pump, as mentioned above.

Figure 8 shows D_{lp}/D_{lm} for all nine experiments, where the predicted geometric mean size of the bedload D_{lp} was computed using the modified Ashida–Michiue relation. The modified Ashida–Michiue relation embodied in Eqs. (10) and (11) is used by Viparelli *et al.* (2010) to evaluate a morphodynamic model for bed aggradation and degradation that includes the evolution of stratigraphy. This model was tested using data from the same flume as was used to develop the modified relation. Note, however, that the modified Ashida–Michiue relation was, like the majority of the bedload relations, developed using data for equilibrium conditions, whereas the numerical model pertains to non-equilibrium conditions. The choice of an equilibrium bedload transport relation to compute the non-equilibrium bedload transport rate in the numerical simulations presented by Viparelli *et al.* (2010) is justified by the common practice to assume that the load relations derived for conditions of equilibrium are also valid for sufficiently slowly-varied non-equilibrium conditions (Parker 2004).

7 Conclusions

Laboratory experiments with a poorly-sorted sand-gravel mixture were performed in a water-feed and sediment-recirculating flume. During the experiments, longitudinal profiles were periodically recorded. As the bed elevation became relatively constant in time throughout the measuring reach, it was assumed that the flow and the sediment transport had reached equilibrium. At this time, the bedload transport rate and its grain size distribution were measured and the run was terminated. Nine different conditions of equilibrium were reached using different values of water discharge and water surface elevation at the downstream flume end. The surface layer was sampled at the end of each run, and grain size distributions of both bedload and the surface layer were computed. At the end of the last experiment, core samples were taken from the bed to measure the vertical stratigraphy of the deposit. Sieve analysis revealed that the bedload had a grain size distribution similar to the initial mixture in all but two runs, in which the bedload was finer than the initial mixture. The bed surface material was, however, significantly coarser than the initial mixture in each run. The upper substrate layers were somewhat coarser than the initial mixture, whereas the deeper layers were similar to the initial mixture. All the experimental data are documented in the Excel file *miniStreamlab.xls* at http://hdl.handle.net/2142/15496.

The experimental results were tested against the bedload relation of Ashida and Michiue (1972). While the relation is not wildly incorrect, it substantially over-predicts the total bedload transport rate, and somewhat under-predicts the geometric mean size of the bedload. With this in mind, a modified surface-based version of the bedload relation of Ashida and Michiue (1972) was fitted to the data. This relation was developed specifically for use in the companion paper to predict the evolution of stratigraphy in a sediment-recirculating flume.

Acknowledgements

This research was funded in part by the National Center for Earth-surface Dynamics, a Science and Technology Center of the US National Science Foundation (EAR-0203296). Special thanks are due to Andrew Waratuke, Marc Killon and Tim Prunkard, who helped greatly with a pump that frequently broke down.

Notation

D = characteristic sediment diameter
F_i = fraction of sediment of active layer in ith size range
g = acceleration of gravity
G_s = bedload transport rate in grams per minute
H = water depth
Q = water discharge
p_i = fraction of bedload material in ith grain size range
q_b = volumetric bedload transport rate per unit width
q_b^* = Einstein parameter = $q_b/[(RgD)^{0.5}D]$
S = bed slope

R = submerged specific sediment gravity
x = streamwise coordinate
α = coefficient in Eq. (12) to fit data
ρ = density of water
σ_{lg} = geometric standard deviation of sediment load
τ_b = shear stress in bed region
τ_b^* = shields parameter = $\tau_b/(\rho RgD)$
τ_c^* = critical value of Shields parameter
ξ_w = water elevation at downstream flume end set by tail gate

References

Ashida, K., Michiue, M. (1972). Study on hydraulic resistance and bedload transport rate in alluvial streams. *Trans. Jap. Soc. Civ. Eng.* 206, 59–69 [in Japanese].

Armanini, A., Di Silvio, G. (1988). A one-dimensional model for the transport of a sediment mixture in non-equilibrium conditions. *J. Hydraulic Res.* 26(3), 275–292.

Blom, A., Ribberink, J.S., de Vriend, H.J. (2003). Vertical sorting in bed forms: Flume experiments with a natural and a trimodal sediment mixture. *Water Resour. Res.* 39(2), 1025–1038.

Blom, A., Parker, G., Ribberink, J.S., de Vriend, H.J. (2006). Vertical sorting and the morphodynamics of bedform dominated rivers: An equilibrium sorting model. *J. Geophys. Res.* 11, F01019, 16 pp., doi:10.1029/2006JF000618.

Blom, A. (2008). Different approaches to handling vertical and streamwise sorting in modeling river morphodynamics. *Water Resour. Res.* 44, W03415, 16 pp., doi:10.1029/2006WR005474.

Cui, Y., Parker, G., Paola, C. (1996). Numerical simulation of aggradation and downstream fining. *J. Hydraulic Res.* 34(2), 185–204.

Cui, Y., Parker, G., Braudrick, C., Dietrich, W.E., Cluer, B. (2006a). Dam Removal Express Assessment Models (DREAM) 1: Model development and validation. *J. Hydraulic Res.* 44(3), 291–307.

Cui, Y., Parker, G., Braudrick, C., Dietrich, W.E., Cluer, B. (2006b). Dam Removal Express Assessment Models (DREAM) 2: Sample runs/sensitivity tests. *J. Hydraulic Res.* 44(3), 308–323.

Einstein, H.A. (1950). The bed-load function for sediment transportation in open channel flows. *Tech. Bull.* 1026. U.S. Dept. Army, Soil Conservation Service, Washington DC.

Fripp, J.B. Diplas, P. (1993). Surface sampling in gravel streams. *J. Hydraulic Engng*. 119(4), 473–490.

Hirano, M. (1971). On riverbed variation with armoring. *Proc. Jap. Soc. Civ. Eng.* 195, 55–65 [in Japanese].

Hoey, T.B., Ferguson, R.I. (1994). Numerical simulation of downstream fining by selective transport in gravel bed rivers: Model development and illustration. *Water Resour. Res.* 30(7), 2251–2260.

Holly Jr., F.M., Rahuel, J.L. (1990a). New numerical/physical framework for mobile-bed modeling 1: Numerical and physical principles. *J. Hydraulic Res.* 28(4), 401–416.

Holly Jr., F.M., Rahuel, J.L. (1990b). New numerical/physical framework for mobile-bed modeling 2: Test applications. *J. Hydraulic Res.* 28(4), 545–564.

Garcia, M.H., ed. (2008). *Sedimentation engineering processes*: Measurements, modeling and practice. ASCE Manuals and Reports on Engineering Practice 110. ASCE, Reston VA.

Ganti, V., Singh, A., Passalacqua, P., Foufoula-Georgiou, E. (2009). Subordinated Brownian motion model for sediment transport. *Physical Review* E 80, 1539-3755/2009/801/011111(9).

Klingeman, P.C., Chaquette, C.J., Hammond, S.B. (1979). Bed material characteristics near Oak Creek Sediment Transport Research Facilities, 1978–1979. *Oak Creek Sediment Transport Report* BM3. Water Resour. Res. Institute, Oregon State University, Corvallis OR.

Meyer-Peter, E., Müller, R. (1948). Formulas for bed-load transport. Proc. 2nd *IAHR Congress*, Stockholm, Sweden, 39–64.

Parker, G., Dhamotharan, S., Stefan, S. (1982a). Model experiments on mobile paved gravel bed streams. *Water Resour. Res.* 18(5), 1395–1408.

Parker, G., Klingeman, P. (1982b). On why gravel bed streams are paved. *Water Resour. Res.* 18(5), 1409–1423.

Parker, G. (1990). Surface-based bedload transport relation for gravel rivers. *J. Hydraulic Res*. 28(4), 417–436.

Parker, G. (1991a). Selective sorting and abrasion of river gravel 1: Theory. *J. Hydraulic Engng*. 117(2), 131–149.

Parker, G. (1991b). Selective sorting and abrasion of river gravel 2: Applications. *J. Hydraulic Engng.* 117(2), 150–171.

Parker, G., Wilcock, P.R. (1993). Sediment feed and recirculating flumes: A fundamental difference. *J. Hydraulic Engng.* 119(11), 1192–1204.

Parker, G., Paola, C., Leclair, S. (2000). Probabilistic Exner sediment continuity equation for mixtures with no active layer. *J. Hydraulic Engng.* 126(11), 818–826.

Parker, G. (2004). 1D sediment transport morphodynamics with applications to rivers and turbidity currents. http://vtchl.uiuc.edu/people/parkerg/morphodynamics_e-book.htm

Parker, G. (2008). Transport of gravel and sediment mixtures. *Sedimentation engineering processes*: Measurements, modeling and practice 3, 165–251, M.H. Garcia, ed. ASCE, Reston VA.

Ribberink, J.S. (1987). Mathematical modelling of one-dimensional morphological changes in rivers with non-uniform sediment. *PhD thesis*. Delft University, Delft NL.

Seal, R., Paola, C., Parker, G., Southard, J.B., Wilcock, P.R. (1997). Experiments of downstream fining of gravel: narrow-channel runs. *J. Hydraulic Engng.* 123(10), 874–884.

Spasojevic, M., Holly Jr., F.M. (1990). 2-D bed evolution in natural watercourses: New simulation approach. *J. Wtrwy., Port, Coast., and Oc. Eng.* 116(4), 425–443.

Singh, A., Fienberg, K., Jerolmack, D.J., Marr, J., Foufoula-Georgiou, E. (2009). Experimental evidence for statistical

scaling and intermittency in sediment transport rates. *J. Geophys. Res.* 114, 0148–0227/09/2007JF000963$09.00.

Toro-Escobar, C.M. Paola, C., Parker, G., Wilcock, P.R., Southard, J.B. (2000). Experiments on downstream fining of gravel 2: Wide and sandy runs. *J. Hydraulic Engng.* 126(3), 35–53.

Vanoni, V.A., ed. (1975). *Sedimentation engineering*. ASCE Manuals and Reports on Engineering Practice 54. ASCE, New York.

Viparelli, E., Sequeiros, O., Cantelli, A., Wilcock, P.R., Parker, G. (2010). River morphodynamics with creation/consumption of grain size stratigraphy 2: numerical model. *J. Hydraulic Res.* 48(6), 727–741.

Wilcock, P.R., McArdell, B.W. (1993). Surface-based fractional transport rates: Mobilization thresholds and partial transport of a sand-gravel sediment. *Water Resour. Res.* 29(4), 1297–1312.

Wilcock, P.R., Crowe, J.C. (2003). Surface-based transport model for mixed-size sediment. *J. Hydraulic Eng.* 129(2), 120–128.

Wilcock, P.R., Orr, C.H., Marr, J.D.G. (2008). The need for full-scale experiments in river science. *Eos*, Trans. AGU 89(1), 1–6.

Wright, S., Parker, G. (2005a). Modeling downstream fining in sand-bed rivers 1: Formulation. *J. Hydraulic Res*. 43(6), 612–619.

Wright, S., Parker, G. (2005b). Modeling downstream fining in sand-bed rivers 2: Application. *J. Hydraulic Res*. 43(6), 620–630.

Wong, M. (2003). Does the bedload equation of Meyer-Peter and Muller fits its own data? Proc. 30th *IAHR Congress*, Thessaloniki, J.F. Kennedy Competition, 73–80.

Wong, M., Parker, G. (2006). Reanalysis and correction of bed-load relation of Meyer-Peter and Müller using their own database. *J. Hydraulic Eng*. 132(11), 1159–1168.

Wong, M., Parker, G., De Vries, P., Brown, T.M., Burges, S.J. (2007). Experiments on dispersion of tracer stones under lower-regime plane-bed equilibrium bedload transport. *Water Resour. Res*. 43(3), 1–23, W03440, doi: 10.1029/2006WR005172.